2020

Soil Structure and Texture Effects on the Precision of Soil Water Content Measurements with a Capacitance-Based Electromagnetic Sensor

Jasreman Singh
University of Nebraska-Lincoln, jasreman.singh@huskers.unl.edu

Derek M. Heeren
University of Nebraska-Lincoln, derek.heeren@unl.edu

Daran Rudnick
University of Nebraska-Lincoln, daran.rudnick@unl.edu

Wayne Woldt
University of Nebraska - Lincoln, wwoldt1@unl.edu

Geng Bai
University of Nebraska-Lincoln, gbai2@unl.edu

See next page for additional authors

Authors
Jasreman Singh, Derek M. Heeren, Daran Rudnick, Wayne Woldt, Geng Bai, Yufeng Ge, and Joe D. Luck

SOIL STRUCTURE AND TEXTURE EFFECTS ON THE PRECISION OF SOIL WATER CONTENT MEASUREMENTS WITH A CAPACITANCE-BASED ELECTROMAGNETIC SENSOR

J. Singh, D. M. Heeren, D. R. Rudnick, W. E. Woldt, G. Bai, Y. Ge, J. D. Luck

HIGHLIGHTS

- Capacitance-based electromagnetic soil moisture sensors were tested in disturbed and undisturbed soils.
- The uncertainty in estimation of soil water depth was lower using the undisturbed soil sample calibrations.
- The uncertainty in estimation of soil water depletion was lower than the uncertainty in volumetric water content.
- Undisturbed calibration of water depletion quantifies water demand with better precision and avoids over-watering.

ABSTRACT. *The physical properties of soil, such as structure and texture, can affect the performance of an electromagnetic sensor in measuring soil water content. Historically, calibrations have been performed on repacked samples in the laboratory and on* in situ *soils in the field, but little research has been done on laboratory calibrations with intact (undisturbed) soil cores. In this study, three replications each of disturbed and undisturbed soil samples were collected from two soil texture classes (Yutan silty clay loam and Fillmore silt loam) at a field site in eastern Nebraska to investigate the effects of soil structure and texture on the precision of a METER Group GS-1 capacitance-based sensor calibration. In addition, GS-1 sensors were installed in the field near the soil collection sites at three depths (0.15, 0.46, and 0.76 m). The soil moisture sensor had higher precision in the undisturbed laboratory setup, as the undisturbed calibration had a better correlation [slope closer to one, $R^2_{undisturbed}$ (0.89) > $R^2_{disturbed}$ (0.73)] than the disturbed calibrations for the Yutan and Fillmore texture classes, and the root mean square difference using the laboratory calibration ($RMSD_L$) was higher for pooled disturbed samples (0.053 m^3 m^{-3}) in comparison to pooled undisturbed samples (0.023 m^3 m^{-3}). The uncertainty in determination of volumetric water content (θ_v) was higher using the factory calibration ($RMSD_F$) in comparison to the laboratory calibration ($RMSD_L$) for the different soil structures and texture classes. In general, the uncertainty in estimation of soil water depth was greater than the uncertainty in estimation of soil water depletion by the sensors installed in the field, and the uncertainties in estimation of depth and depletion were lower using the calibration developed from the undisturbed soil samples. The undisturbed calibration of soil water depletion would determine water demand with better precision and potentially avoid over-watering, offering relief from water shortages. Further investigation of sensor calibration techniques is required to enhance the applicability of soil moisture sensors for efficient irrigation management.*

Keywords. *Calibration, Capacitance, Depletion, Irrigation, Precision, Sensor, Soil water content, Structure, Uncertainty.*

Accurate and continuous determination of soil water content helps drive efficient management of irrigation and drainage, making it a key component in irrigation and drainage research (Evett, 2007). Knowledge of irrigation scheduling principles is essential to develop and implement an effective irrigation management plan for each field on a farm. This knowledge can inform the timing and depth of irrigation application, thereby reducing the likelihood of excessive or insufficient irrigation. Soil water quantity is one of the essential geophysical estimates needed for implementation of deficit irrigation, which helps to manage crop water status to maximize yield with a limited water supply (Geerts and Raes, 2009). To maximize yield from a given farm area when the water supply is adequate, an appropriate irrigation scheduling strategy is to prevent crop water stress throughout the growing season and avoid excess water application. However, with an inad-

Submitted for review in November 2019 as manuscript number NRES 13496; approved for publication as part of the Global Water Security Collection by the Natural Resources & Environmental Systems Community of ASABE in November 2019.

The mention of trade names or commercial products is for information purposes and does not constitute an endorsement or recommendation for use by the University of Nebraska-Lincoln or the authors.

The authors are **Jasreman Singh,** Graduate Research Assistant, **Derek M. Heeren,** Associate Professor and Irrigation Engineer, Daugherty Water for Food Global Institute (DWFI) Faculty Fellow, **Daran R. Rudnick,** Assistant Professor and Irrigation Management Specialist, DWFI Faculty Fellow, **Wayne E. Woldt,** Associate Professor and Environmental Engineer, DWFI Faculty Fellow, **Geng Bai,** Research Assistant Engineer, **Yufeng Ge,** Associate Professor and Advanced Sensing Systems Engineer, DWFI Faculty Fellow, and **Joe D. Luck,** Associate Professor and Precision Agriculture Engineer, DWFI Faculty Fellow, Department of Biological Systems Engineering, University of Nebraska, Lincoln, Nebraska. **Corresponding author:** Derek M. Heeren, 241 Chase Hall, University of Nebraska, Lincoln, NE 68583-0726; phone: 402-472-8577; e-mail: derek.heeren@unl.edu.

  ISSN 2151-0032 https://doi.org/10.13031/trans.13496

equate water supply, it is challenging to manage the distribution of irrigation throughout the growing season to attain the best possible yield (Martin et al., 1990).

Soil volumetric water content (θ_v) quantifies the amount of water in soil. The available water-holding capacity of the soil (the amount of water available to the plants) is the water held between field capacity (FC) and permanent wilting point (PWP), i.e., the upper and lower limits of water available to the plants. FC is often defined as the soil water content of a previously saturated soil after 24 h of free drainage into the underlying soil, and PWP is the soil water content at which the crop wilts and cannot recover even if irrigated. In addition, a crop needs to be irrigated before the available water is totally depleted because the crop will have already been subjected to substantial water stress (and yield loss). Therefore, the management-allowed depletion (MAD) concept is often used, which initiates irrigation when the soil water has decreased to a specific θ_{MAD} level (Evett, 2007). MAD is a management technique involving a maximum soil water extraction to prevent yield reduction due to water stress. The θ_{MAD} level varies depending on soil type, rooting depth, crop sensitivity to water stress, time of season, characteristics of the irrigation system, and other factors (Martin et al., 1990). The θ_{MAD} level is typically selected so that the soil never becomes dry enough to limit plant growth and yield, although in some situations it may be a drier level that allows development of some plant stress. Irrigation application is commonly initiated at a θ_v higher than θ_{MAD} due to error in θ_v measurement that may result in unintended crop stress.

Electromagnetic (EM) sensors are widely used in agricultural research and production settings. These sensors gather information about soil, crop, and climatic parameters at a high spatial and temporal resolution and can be a part of wireless sensor network systems. Sensor data provide insights into agricultural processes governing crop growth, soil water, and nutrient use and can help with timely and informed decisions for management practices. EM sensors have found wide application in monitoring θ_v because of the various advantages they offer, which include easy installation, high cost-effectiveness, lesser regulatory and safety concerns (compared to neutron moisture meters), and continuous measurement (Varble and Chávez, 2011). However, factors such as soil temperature, apparent electrical conductivity, textural composition, organic matter content (OMC), and bulk density can influence soil θ_v (Baumhardt et al., 2000; Kelleners et al., 2004; Namdar-Khojasteh et al., 2012; Paige and Keefer, 2008; Singh et al., 2019; Vaz et al., 2013), and these factors may not be considered in the factory calibration of EM sensors. Factory calibrations were described by Hignett and Evett (2008) as being "commonly performed in a temperature controlled room, with distilled water and in easy to manage homogeneous soil materials (loams or sands) which are uniformly packed around the sensor." The field conditions in which EM sensors are installed might differ from these controlled conditions, which may reduce the applicability of factory calibrations (Hignett and Evett, 2008).

While time domain reflectometry (TDR) is regarded as the one of the most accurate methods to determine θ_v (Dobriyal et al., 2012), sensors based on capacitance and frequency domain technology offer more practical and cost-effective alternatives to TDR sensors. The performance of EM soil water sensors under various soil conditions has been investigated extensively (Geesing et al., 2004; Mittelbach et al., 2012; Singh et al., 2018; Varble and Chávez, 2011; Vaz et al., 2013), and some studies have proposed correcting for non-water influences on θ_v by developing soil-specific calibrations. For soil moisture sensors based on capacitance and frequency domain technology, the sensor response over a large θ_v range has been captured in the laboratory (Adeyemi et al., 2016; Goswami et al., 2019; Ojo et al., 2015; Provenzano et al., 2016; Santhosh et al., 2017) and in the field (Datta et al., 2018; Huang et al., 2017; Lea-Cox et al., 2018; Ojo et al., 2014; Rudnick et al., 2015; Sui, 2017).

Sensor calibrations for different soil textures have generally been conducted using soil with a disturbed structure in a laboratory and using soil with an undisturbed structure in the field. However, there is a lack of research evaluating whether there is a difference in the calibration responses for disturbed and undisturbed soil samples in the same conditions to determine whether the relationship between sensor output and actual θ_v is truly different in disturbed versus undisturbed soil, in which case the calibration environment may need to match the intended soil environment. Manufacturers' calibrations for soil moisture sensors are typically based on the response of these sensors in disturbed soil samples, whereas undisturbed soil samples capture the structure of soil in the field. Investigation of an undisturbed soil sample in a laboratory setting would allow a more controlled experiment, e.g., complete saturation, drying, and determination of θ_v by gravimetric method, compared to calibration in the field. In addition, this comparison might guide us toward better calibration procedures for soil moisture sensors as well as a better understanding of the influence of soil structure on the calibration of these sensors.

The specific objectives of this research were to (1) evaluate the differences in responses of soil moisture sensors installed in varying soil structure (disturbed and undisturbed) and texture conditions and (2) assess the uncertainty involved in field irrigation scheduling based on depletion as well as management based on volumetric water content (θ_v).

Materials and Methods

Site and Soil Description

A laboratory study was conducted to analyze the performance of a recently developed EM soil moisture sensor using capacitance and frequency domain technology in two different soil classes. The soil used in the experiment was collected from a specified depth (0.08 to 0.23 m) at two sites across a center-pivot irrigated field in Mead, Nebraska. The soil collection sites in the field were occurrences of Fillmore (fine, smectic, mesic Vertic Argiabolls) and Yutan (fine-silty, mixed, superactive, mesic Mollic Hapludalfs). According to the USDA National Resources Conservation Service (NRCS) classification system, the corresponding texture classes were silt loam and silty clay loam, respectively.

SENSOR DESCRIPTION

A recently developed capacitance and frequency domain technology based sensor (GS-1, METER Group, Pullman, Wash.) was used for this study. The GS-1 sensor is configured with two parallel rods (5.2 cm in length) that serve as the waveguide. The sensor head contains the necessary firmware and electronics, which generate an electromagnetic field in the surrounding medium to measure the dielectric constant. The sensor is designed to use an oscillator running at 70 MHz that charges in response to the dielectric constant of the surrounding material. The measured dielectric constant is correlated to the apparent permittivity, which is correlated to θ_v. The charge value (mV) provided by the sensor is related to θ_v of the measurement volume using the manufacturer's equation:

$$\theta_v = 4.94 \times 10^{-4} \times \text{mV} - 0.554 \quad (1)$$

The GS-1 sensor has the capability to remain in the soil for a long time and has a measurement volume of 430 mL (fig. 1). A datalogger (CR1000, Campbell Scientific, Inc., Logan, Utah) was used to report θ_v.

EXPERIMENT DESCRIPTION

Three vertical soil columns for each disturbed and undisturbed soil sample (fig. 1) were constructed for each of the two soil collection sites (12 samples total). Each soil column was contained in a separate polyvinyl chloride (PVC) pipe section (0.203 m length by 0.152 m internal diameter). The PVC pipe section was beveled from one side and then hammered vertically into the soil with the beveled side at the bottom using a soil hammer that had a metallic plate at the base slightly larger than the external diameter of the PVC pipe. For each replication, the top 0.076 m of soil was excavated before sample collection.

For undisturbed soil sampling, the PVC pipe was hammered to a depth of 0.102 m into the soil to collect a 0.102 m intact soil core, and the GS-1 sensor was then inserted downward into the soil column until the bottom of sensor head was flush with the top of the column. Subsequently, a 0.050 m layer of the soil was packed over the top of sensor at the same bulk density, resulting in a total core length of 0.152 m. The soil column with undisturbed soil closely mimicked the installation of a sensor in the field; unless inserted directly into the soil surface, the sensor head is inevitably be surrounded by disturbed soil, while the rods are in intact soil.

The soil sampling for disturbed soil was performed by hammering the PVC pipe to a depth of 0.152 m into the soil. The PVC pipe was then excavated from the ground, leveled, and the bottom end of the pipe was covered with landscape fabric and window screen to create a water-permeable but soil-impermeable barrier. The soil column was then transported to the laboratory, where the soil was extracted from the PVC pipe, oven-dried at 40°C to 45°C for 48 h, ground, passed through a 2 mm sieve, and then repacked into the PVC pipe at the same bulk density (as shown in table 1 for both soil texture classes) to a height of 0.152 m, with the sensor installed at 0.102 m from the bottom. The placement of the GS-1 soil moisture sensor and the dimensions of the soil column were carefully designed considering the sensing volume of sensor (fig. 1) so that the sensing volume remained entirely within the column.

As a part of the experiment, the soil columns were subjected to two rounds of saturation and drying to determine the θ_v accuracy of the GS-1 sensor in the two soil structures and texture classes. For each saturation event, the soil columns were allowed to saturate from the bottom up and then allowed to drain briefly before sealing the bottom ends with

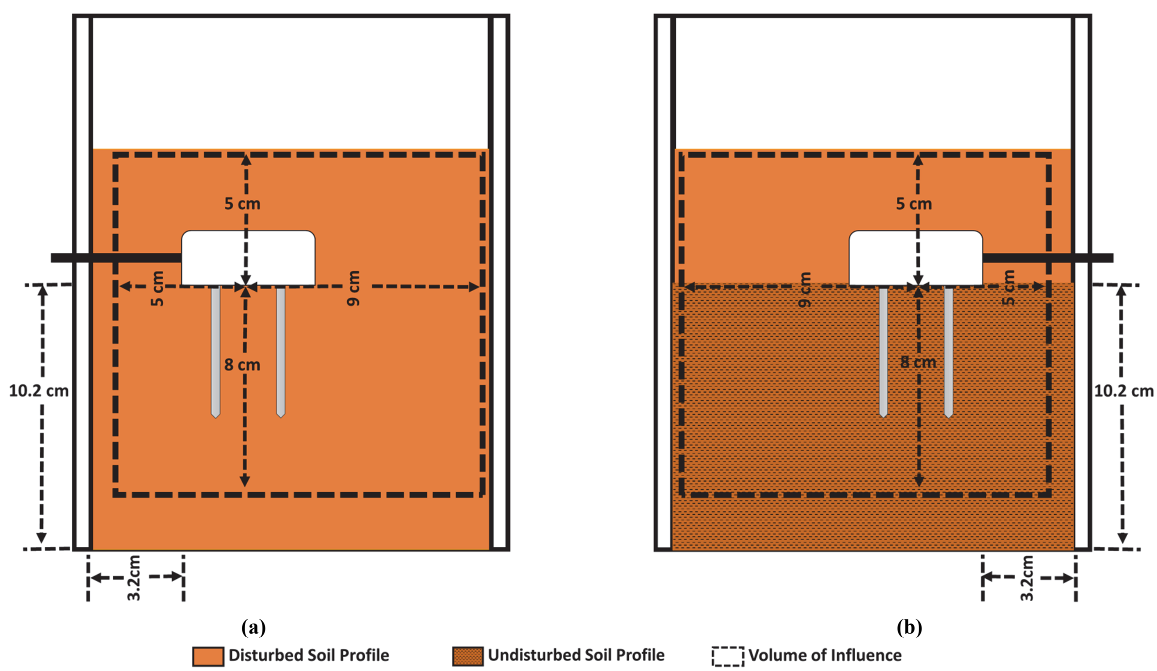

Figure 1. Illustration of GS-1 soil moisture sensor and its maximum volume of influence (dashed rectangle) as reported by Decagon Devices, Inc. (Cobos, 2016) when the sensor was inserted into (a) disturbed and (b) undisturbed vertical soil profile columns. The dimensions of the soil columns and the placement of the sensor were carefully designed so that the sensing volume of the sensor extended within the column.

Table 1. Textural composition, organic matter content (OMC), bulk density (ρ_b), and saturated paste extract electrical conductivity (EC_a) of the soils at the study site as determined from three cores taken from each site. Values are means ± standard deviations.

Soil Type	Sand (%)	Silt (%)	Clay (%)	OMC (%)	ρ_b (g cm^{-3})	EC_a (dS m^{-1})
Yutan	19	46	35	3.8	1.35	0.24
	±2	±2	±2	±0.0	±0.06	±0.02
Fillmore	17	47	37	4.4	1.29	0.41
	±1	±1	±1	±0.1	±0.02	±0.03

plastic, which prevented further drainage. All replicates showed shrinking of the soil following saturation, but the change in height (or volume) was less than 4% of the initial height and was considered insignificant. All data used for calculating θ_v were collected after the shrinking had occurred. The soil columns were then loaded onto a portable trolley and stored in a temperature-controlled room at 40°C to 45°C for drying and water redistribution. The columns were allowed to dry from the top and were covered with plastic on top during the redistribution process, after which the θ_v level was recorded. This process of drying, redistribution, and measurement was repeated to collect data across a range of θ_v.

For field irrigation applications, θ_{MAD} is generally considered to be 50% of the plant-available water of the soil type, as error in θ_v measurement may result in unintended crop stress. The FC (θ_{FC}) for the experimental site (silty clay loam soil) was 40% on average, and 50% MAD was attained at θ_{MAD} of 28% based on past studies (Barker et al., 2017; Lo et al., 2017). Therefore, as a part of the laboratory experiment, the soil was saturated initially and then readings were taken from θ_v of 41.5% to 28%, recording the weight at increments of 1.5% θ_v.

It was important to allow adequate time for the water redistribution process to ensure that θ_v was nearly uniform across the soil column and the sensing volume of the GS-1, and this process required more time at low θ_v (resulting in low unsaturated hydraulic conductivity). Therefore, before the laboratory experiment, the drying and redistribution processes were simulated with a model for one-dimensional transient water flow in porous media (HYDRUS-1D, PC Progress, Prague, Czech Republic). The default parameters for a silty clay loam soil (which closely resembled the soil texture of the samples) were used with a no-flux boundary condition for the lower boundary. The upper boundary condition was "atmospheric boundary condition with surface layer" for drying and a no-flux boundary condition for redistribution. The time interval for each step of drying and redistribution in the laboratory experiment was determined based on the HYDRUS output. HYDRUS simulated the total drying cycle to be 23 days. The simulation involved drying the soil core from θ_{sat} to θ_v = 41.5%, allowing the profile to redistribute to a uniform θ_v, drying to θ_v = 40%, allowing it to redistribute, and continuing in increments ($\Delta\theta_v$ = 1.5%) to a final θ_v of 28%. The frequency of weighing the soil columns ranged from twice a day to once every three to four days as the evaporation rate decreased near the end of the drying cycle.

The output of the GS-1 sensors was collected and reported every minute with a datalogger (CR1000, Campbell Scientific, Logan, Utah) throughout each drying cycle. A weighing balance (TR-8102D, Denver Instrument Co., Bohemia, N.Y.) with an accuracy of 0.1 g was used to weigh each soil column. At the end of the entire experiment, the soil from each soil column was extracted and oven-dried at 105°C for approximately 48 h to determine the final θ_v and to back-calculate the actual θ_v (reference θ_v) for the entire cycle. The weight of the empty column setup, including the sensor, was determined in the same manner as when the column contained soil.

Analysis

To evaluate the accuracy of θ_v measurement by the GS-1 sensors in disturbed and undisturbed soil samples in the two different soil types, the sensor-reported θ_v output was compared to the reference θ_v determined from the soil column weight. The reference θ_v at each weighing time was determined using equation 2 and was compared to the sensor-reported θ_v at the closest time stamp:

$$\text{Reference } \theta_v = \frac{w_{total} - w_{soil} - w_{setup}}{\rho_w V_{soil}} \tag{2}$$

where w_{total} is the total weight of the soil column, w_{soil} is the weight of dry soil in the column, w_{setup} is the weight of the column setup without soil, ρ_w is the density of water (≈1 g cm^{-3}), and v_{soil} is the volume of soil in the column.

The absolute magnitude of differences between sensor θ_v and reference θ_v while penalizing larger differences was indicated by the root mean square difference ($RMSD_F$) for each analysis group (soil structure, soil type, and structure-type combinations):

$$RMSD_F = \sqrt{\frac{\sum_t^n \sum_i^m \left(\theta_{i,t}^F - \theta_{i,t}^R\right)^2}{mn}} \tag{3}$$

where $RMSD_F$ is the RMSD using the factory calibration, n is the number of times the columns were weighed during the drying cycle, t is the index of the weighing time, m is the number of soil columns per analysis group, i is the index of the soil column, $\theta^F_{i,t}$ is the sensor-reported θ_v (using the factory calibration) of the ith column at weighing time t, and $\theta^R_{i,t}$ is the reference θ_v of the ith column at weighing time t. There were three columns (replicates) for each soil type-structure combination, six columns for a pooled analysis of all columns with a given soil structure, and six columns for a pooled analysis of each soil type. The $RMSD_F$ was also calculated for each replicate (m = 1 with multiple data points in time).

Because the $RMSD_F$ was based on the error between sensor θ_v using the factory calibration and true θ_v determined with the gravimetric method, it was used to quantify the uncertainty associated with using the GS-1 sensor with the factory calibration, without performing a calibration specific to that particular sensor or soil type. To simulate a scenario in

which the sensor was calibrated in the laboratory for a specific soil type, the $RMSD_L$ was used to quantify the uncertainty:

$$RMSD_L = \sqrt{\frac{\sum_t^n \sum_i^m \left(\theta_{i,t}^L - \theta_{i,t}^R\right)^2}{mn}} \quad (4)$$

where $RMSD_L$ is the RMSD using a soil-specific laboratory calibration, and $\theta^L_{i,t}$ is the θ_v from the sensor (using the laboratory calibration) of the *i*th column at weighing time *t*.

The effect of soil structure (disturbed and undisturbed) on the θ_v measurement accuracy of the GS-1 sensor was analyzed. Analysis of variance (ANOVA) with a significance level of $\alpha = 0.05$ was conducted using R (R Foundation for Statistical Computing, Vienna, Austria) on the 12 weighing times from the drying cycle. The effect of the different soil types (Fillmore and Yutan) on sensor θ_v accuracy was also analyzed. Implications for irrigation management were also assessed.

Results and Discussion

Analysis Based on Variable Soil Structure

A laboratory study was conducted to analyze the performance of the recently developed capacitance and frequency domain based GS-1 soil moisture sensor operating at 70 MHz in two different soil structures (disturbed and undisturbed). For the analyses in disturbed and undisturbed soil structures, both soil texture classes were considered, i.e., the datasets for the disturbed and undisturbed soil structures both comprised samples of Yutan and Fillmore soils. The equations in figure 2 were tested statistically, and it was found that linear equations were statistically significant ($p < 0.05$) for both disturbed and undisturbed soil samples. In addition, the linear calibration equations for disturbed and undisturbed soil samples reported in this study were found to be significantly different from each other ($p = 8.65 \times 10^{-6}$). For the disturbed soil samples, an underestimation of sensor-reported θ_v was observed at higher θ_v, and an overestimation of sensor-reported θ_v was observed at lower θ_v. However, for the undisturbed soil samples, an overestimation of sensor-reported θ_v was noted throughout the θ_v range, with a slight underestimation of sensor-reported θ_v at higher θ_v. The coefficient of determination (r^2) for the undisturbed soil columns, which mimicked the field conditions, was 0.89, whereas the r^2 for the disturbed soil columns, which represented the laboratory conditions, was 0.73.

Similar results have been observed in previous investigations of the performance of a frequency domain reflectometry sensor. Ojo et al. (2015) found that the results of field calibration of the sensor were superior ($r^2 = 0.95$) to the laboratory calibration ($r^2 = 0.89$). On the contrary, Gabriel et al. (2010) found that the accuracy of a capacitance probe (EnviroScan, Sentek Pty Ltd., Kent Town, South Australia) was slightly better under field conditions using laboratory calibration equations (RMSD = 0.019 m^3 m^{-3}) rather than field conditions (RMSD = 0.023 m^3 m^{-3}) and recommended the use of laboratory conditions because they are easily reproducible, facilitate work planning, and minimize uncertainties. The literature has shown that capacitance and frequency domain sensors (EC-5 and ECH_20) operating at the same scaled frequency (70 MHz) have low sensitivity to confounding soil environmental factors such as soil texture, bulk electrical conductivity, and temperature (Kizito et al., 2008).

The results from this study (fig. 2) indicate that the sensor-reported θ_v in the undisturbed soil structure had better correlation (slope for undisturbed soil samples was closer to one) with the reference θ_v when compared to the disturbed soil structure, and the uncertainty in θ_v determination was higher using the factory calibration ($RMSD_F$; table 2) in comparison to the laboratory calibration ($RMSD_L$; table 2). The $RMSD_L$ for disturbed and undisturbed soil samples based on fitted values from the calibration equation was 0.053 and 0.028 m^3 m^{-3}, respectively (table 2). For the capacitance-based GS-1 soil moisture sensor used in this study, higher accuracy was observed with undisturbed soil samples ($RMSD_F$ = 0.074 m^3 m^{-3}) in comparison to disturbed samples ($RMSD_F$ = 0.050 m^3 m^{-3}) for the two soil types (Yutan silty clay loam and Fillmore silt loam). On the contrary, Majone et al. (2013) found out that for Meter Environment's EC-5

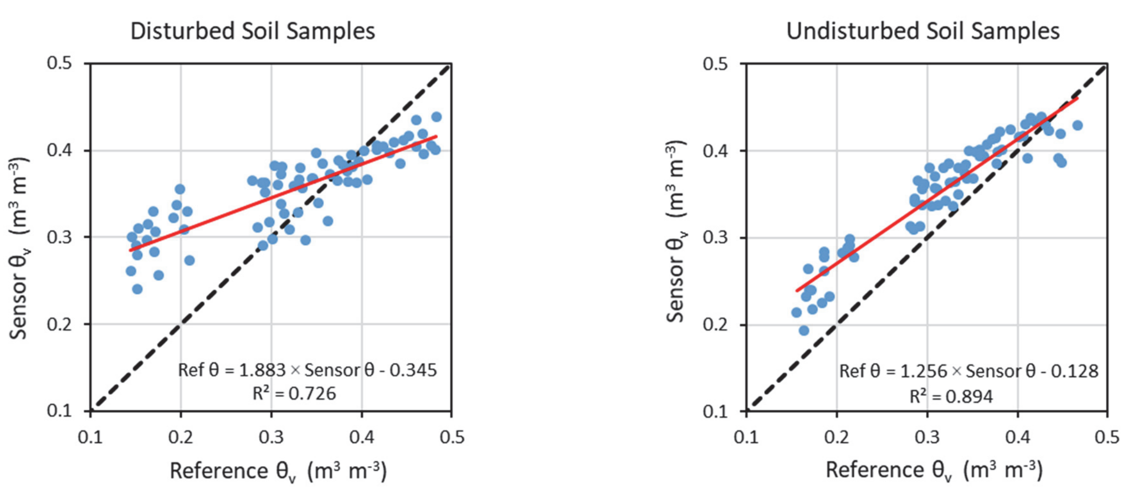

Figure 2. Response of GS-1 soil moisture sensor to different soil structures (disturbed and undisturbed) during the experiment. Both soil texture classes (Yutan and Fillmore) were considered for the disturbed and undisturbed soil samples.

Table 2. RMSD ($m^3 m^{-3}$) from GS-1 laboratory experiments (eqs. 3 and 4) and error (cm) used for error bars (figs. 5 and 6).

	Disturbed Soil Structure						Undisturbed Soil Structure					
$RMSD_F$	0.074						0.050					
$RMSD_L$	0.053						0.028					
	Yutan silty clay loam			Fillmore silt loam			Yutan silty clay loam			Fillmore silt loam		
$RMSD_F$	0.065			0.082			0.056			0.043		
$RMSD_L$	0.046			0.036			0.028			0.024		
Root zone water depth error	0.046 × 100 cm = 4.6 cm			0.036 × 100 cm = 3.6 cm			0.028 × 100 cm = 2.8 cm			0.024 × 100 cm = 2.4 cm		
	Rep 1	Rep 2	Rep 3	Rep 1	Rep 2	Rep 3	Rep 1	Rep 2	Rep 3	Rep 1	Rep 2	Rep 3
$RMSD_F$	0.076	0.052	0.064	0.086	0.070	0.089	0.048	0.055	0.064	0.047	0.046	0.035
$RMSD_L$	0.006	0.007	0.008	0.006	0.008	0.007	0.006	0.009	0.006	0.005	0.005	0.007
Root zone depletion error	0.006 × 100 cm = 0.6 cm			0.007 × 100 cm = 0.7 cm			0.006 × 100 cm = 0.6 cm			0.005 × 100 cm = 0.5 cm		

(a capacitance-based soil moisture sensor), the sensor's accuracy improved when the sensor was calibrated with the site soil in the laboratory prior to deployment at the field site. However, Logsdon (2009) concluded that field as well as laboratory calibration should be conducted for soil moisture probes that operate at MHz frequencies to identify discrepancies and make required corrections.

Analysis Based on Variable Soil Texture

In addition to investigating the sensor response in different soil structures, the sensor response was analyzed in two different textured soils (Yutan silty clay loam and Fillmore silt loam). For each soil structure (disturbed and undisturbed), three replications each of Yutan and Fillmore were studied along with the interaction effects of soil texture and structure. Linear calibration equations were statistically significant ($p < 0.05$) for Yutan and Fillmore in both disturbed and undisturbed soil structures (fig. 3). Calibration of θ_v as related to the analysis based on variable soil texture was slightly different for Yutan and Fillmore in both disturbed and undisturbed soil structures. Overestimation of sensor-reported θ_v at lower θ_v was higher in Fillmore in comparison

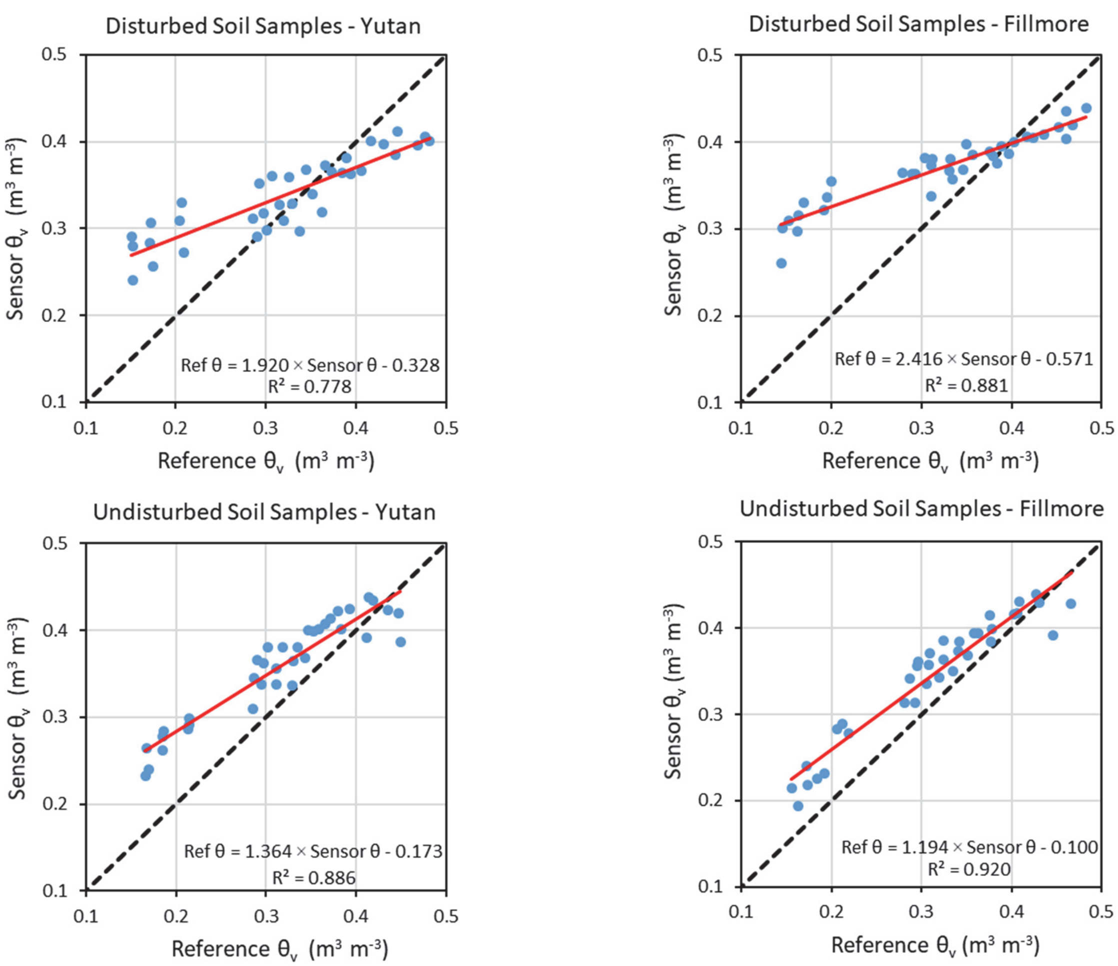

Figure 3. Response of GS-1 soil moisture sensor to different soil texture classes (Yutan silty clay loam and Fillmore silt loam) in disturbed and undisturbed soil structures during the experiment.

to Yutan, and underestimation of sensor-reported θ_v at higher θ_v was higher in Yutan in comparison to Fillmore in the disturbed soil structure. Overestimation and underestimation of sensor-reported θ_v was higher at lower and higher θ_v ranges, respectively, for Yutan in comparison to Fillmore. The correlation was better (slope closer to one) for undisturbed soil samples than for disturbed soil samples in both Yutan and Fillmore soil types.

The reported $RMSD_L$ based on fitted values from the calibration equations was found to be 0.046 and 0.036 $m^3\ m^{-3}$ for Yutan and Fillmore, respectively, in disturbed soil structures (table 2). On the other hand, for undisturbed soil structures, the reported $RMSD_L$ was 0.028 and 0.024 $m^3\ m^{-3}$ for Yutan and Fillmore, respectively (table 2). On the contrary, Haberland et al. (2014) observed that the manufacturer's calibration for a frequency domain reflectometry capacitance probe (Diviner 2000) proved to be quite precise and accurate in laboratory conditions compared to field conditions for clay loam and clay soils. In addition, Provenzano et al. (2016) found out that the calibration for undisturbed soil columns assessed in the laboratory was characterized by lower errors than the calibration for undisturbed soil columns assessed in the field using a Diviner 2000 in seven different soils. The calibration equations for Yutan and Fillmore in disturbed soil structures were significantly different ($p = 0.0398$). Groves and Rose (2004) also concluded that the calibration equations for different soil types, as determined with a Diviner 2000, were different in a laboratory setup. However, in the undisturbed soil structure, the response of the GS-1 sensor for Yutan and Fillmore soil types was not significantly different ($p = 0.1$).

Some studies have reported insensitivity of capacitance probe response to soil texture. For example, Andrade-Sánchez et al. (2004) observed that the response of a capacitance-based soil moisture sensor was not affected by soil texture when it was tested under static conditions in Yolo loam, Capay clay, and Metz sand soils. Similarly, Francesca et al. (2010) found that capacitive sensors (ECH$_2$O, and EC-5) could be used in clay loam and loam soils with the same calibration equation, independent of depth, with $RMSD_L$ ranging between 0.025% and 0.036%. Our results imply that the response of a capacitance-based soil moisture sensor could be similar for different soil types with an undisturbed structure while being different in a disturbed structure. We did not include a swelling clay soil in our experiment, which may have required an equation significantly different from that for the other soil types.

In addition, the interaction of soil texture in disturbed and undisturbed soil structures was analyzed. For the Yutan soil, the sensor response was significantly different ($p = 0.0036$) between the disturbed and undisturbed soil structures. Similarly, for the Fillmore soil, the response was different ($p = 1.46 \times 10^{-11}$) between the disturbed and undisturbed soil structures. Furthermore, the uncertainty in θ_v determination was higher using the factory calibration ($RMSD_F$; table 2) in comparison to the laboratory calibration ($RMSD_L$; table 2) for the different soil structures, texture classes, and across all replications.

Implications for Irrigation Management

Data from GS-1 soil moisture sensors *in situ* at the location of the soil sampling sites were collected for an uncertainty analysis for use in irrigation scheduling. Previously, Datta et al. (2018) suggested that GS-1 sensors presented acceptable accuracies for managing irrigation at sites with low salinity and low clay content based on the reported root mean square errors. In the current study, the capacitance-based GS-1 sensors were installed and monitored for the 2018 growing season at depths of 0.15, 0.46, and 0.76 m. The temporal trends (fig. 4) suggested that the shallower depths (0.15 and 0.46 m) were more sensitive to wetting events such as irrigation or precipitation, as is evident from the upward spikes for the shallower depths. The changes in soil moisture at the deeper depth (0.76 m) were gradual and the range of moisture depletion was fairly small in comparison to shallower depths.

Root zone water depth is the equivalent depth of water in the soil and is the product of θ_v and thickness of the soil layer. The root zone water depth for the top 1 m profile (fig. 5) was determined using the weighted-average method from the θ_v observed by the GS-1 sensors installed at 0.15, 0.46, and 0.76 m depths for each site location (Yutan and Fillmore). Both FC and PWP were estimated based on texture with a pedotransfer function (Saxton and Rawls, 2006), which is a common recommendation for irrigation management. In addition, the 50% MAD was considered as a base-

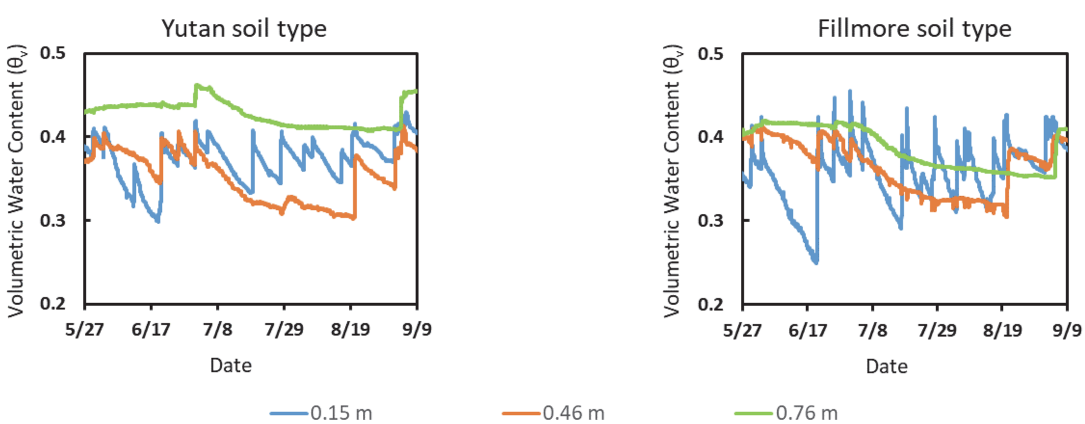

Figure 4. Temporal trends (2018 growing season) in soil moisture reported by GS-1 sensors installed at 0.15, 0.46, and 0.76 m depths using the manufacturer's calibrations for the sites of soil collection (Yutan silty clay loam and Fillmore silt loam).

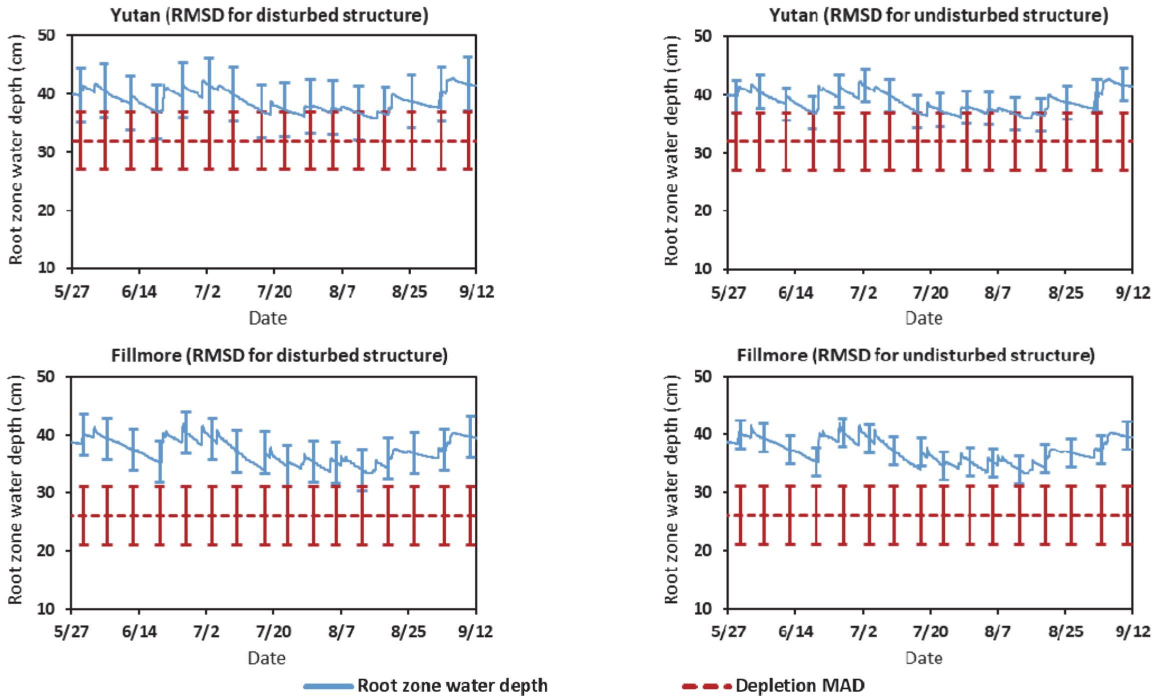

Figure 5. Temporal trends (2018 growing season) in root zone water depth (cm) for the top 100 cm profile reported by GS-1 sensors for the two soil sampling locations (Yutan silty clay loam and Fillmore silt loam) along with vertical error bars (level of uncertainty) determined from disturbed and undisturbed soil structure calibrations for each soil type. The vertical error bars for the MAD water depth were determined from RMSD for both θ_{FC} and θ_{WP} from Saxton and Rawls (2006).

line for comparison and was calculated using the pedotransfer function FC and PWP for a silty clay loam and silt loam.

The error bars shown in figure 5 for the root zone water depth from the GS-1 sensors and the MAD illustrate the uncertainty in the data when used for irrigation management. The GS-1 error bars were determined from the $RMSD_L$ from the laboratory experiment for each soil structure and soil texture type (table 2). The error bars indicate the degree of uncertainty for soil moisture reported by the GS-1 sensors when using the disturbed calibration. This is a conservative estimate of uncertainty because producers typically use the factory calibration, which would have a larger uncertainty ($RMSD_F$, table 2). It can be seen that the uncertainty for root zone water depth estimation from the GS-1 sensor calibration was less for the undisturbed soil structure in comparison to the disturbed soil structure. On the other hand, the error bars for water depth at MAD were calculated from RMSD for both θ_{FC} and θ_{WP} from Saxton and Rawls (2006) (error bar = 0.05 × 100 cm = 5 cm). The large error bars for both water depth and MAD water depth would make it difficult to manage irrigation precisely (fig. 5); the soil would need to remain quite wet to ensure that it did not get drier than the MAD water depth (accounting for uncertainty in both the MAD estimate and the soil water measurement).

Measurement of FC would reduce some of the uncertainty associated with using a pedotransfer function; however, determination of FC is complex and tedious, as it can change with soil texture and soil layering (Romano and Santini, 2002), and measuring FC is not practical for irrigation managers (King et al., 2006). However, measurement of observational field capacity (FC_{obs}), an estimate of FC in the field under non-experimental conditions, is relatively easy and feasible for producers. Martin et al. (1990) demonstrated that "good indication of the field capacity water content can be determined by sampling field soils one to three days after a thorough irrigation or rain and when crop water use is small." This suggestion is consistent with the concept of FC_{obs} (Lo et al., 2017). In this study, the FC_{obs} was determined for the Yutan and Fillmore soil types from the graph of temporal trends in root zone water depth from the *in situ* GS-1 data (fig. 4). The FC_{obs} for the root zone was determined to be 0.40 and 0.37 $m^3\ m^{-3}$ for the Yutan and Fillmore soil types, respectively. This removes the uncertainty associated with the difference between actual FC and pedotransfer function FC or lab-determined FC.

Additionally, irrigation can be managed using the root zone depletion (D) instead of the root zone water depth. The D is the amount of water that has been depleted below the FC_{obs}:

$$D = d_{rz}\left(\theta_{FC,obs} - \theta_v\right) \quad (5)$$

where D is the root zone depletion (cm), d_{rz} is the depth of the root zone (cm), and $\theta_{FC,obs}$ is the volumetric water content ($m^3\ m^{-3}$) associated with the FC_{obs}. The D was determined for the top 100 cm profile (fig. 6) using the weighted-average method from the soil moisture observed by the GS-1 sensors installed at 0.15, 0.46, and 0.76 m depths for each soil sampling location (Yutan and Fillmore). The D associated with 50% MAD (D_{MAD}) was determined from the PWP for silty clay loam and silt loam soil types from Saxton and Rawls (2006) and the FC_{obs} from the GS-1 data.

Managing irrigation based on D instead of θ_v has three advantages. First, it removes uncertainty from the spatial

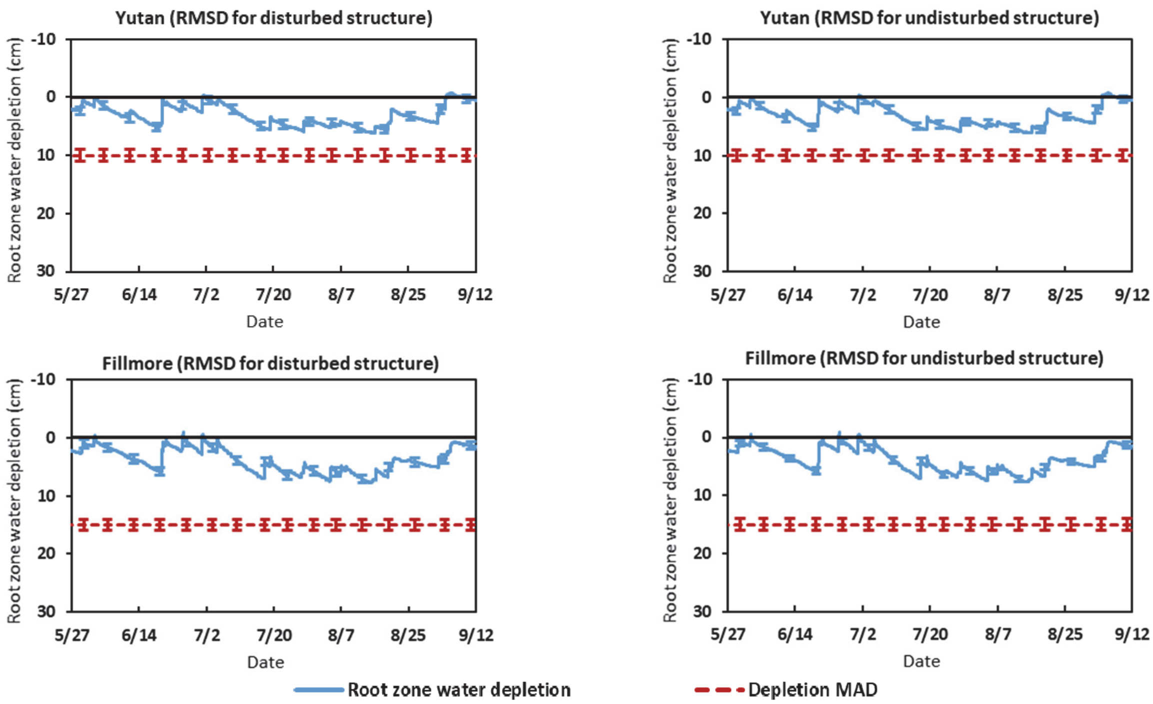

Figure 6. Temporal trends in root zone depletion (cm) for the top 100 cm (1 m) profile reported by GS-1 sensors for the soil collection sites (Yutan silty clay loam and Fillmore silt loam) along with vertical error bars determined from the median (from three replications) of disturbed and undisturbed soil structure calibrations for the two soil types during the 2018 growing season.

variability of θ_{FC}, particularly in subhumid or humid climates where the growing season starts at $D = 0$ throughout the field regardless of the FC at each location. Second, it removes uncertainty in θ_{FC} because $\theta_{FC,obs}$ is determined by the sensor, and uncertainty is removed when taking the difference of $\theta_{FC,obs}$ and θ_v. Third, it removes sensor-to-sensor variation in sensor response because management is based on the change in water content instead of requiring accurate determination of the magnitude of θ_v. Therefore, the error bars for the *D* (fig. 6) were estimated with the RMSD for a best-case scenario (laboratory calibration) and for only one column (without sensor-to-sensor variability). Specifically, the error bars are the median $RMSD_L$ for each soil structure and soil texture combination (table 2). The error bars for D_{MAD} were calculated from the RMSD for WP (1 cm) from Saxton and Rawls (2006) and assumed that the uncertainty in FC_{obs} was negligible because it was determined *in situ* from the soil water sensor.

When using GS-1 sensors for irrigation scheduling, the uncertainty when managing with *D* (fig. 6) was much lower than the uncertain when managing for θ_v (fig. 5). This approach gives irrigation managers more confidence in determining when and how much to irrigate. The soil water can be managed at a level closer to the MAD threshold, with a small risk of the soil being drier than MAD.

Soil water depletion along with the occurrence of plant water stress, the depth of water applied with each irrigation, and the efficiency and capacity of the irrigation system help drive irrigation scheduling. This scheduling can help minimize the labor cost involved (if any) and undesirable leaching, as it identifies the earliest date for irrigation application. The application date is further determined by the net irrigation depth to be applied. If the soil moisture depletion is greater than the net irrigation depth, it will result in drainage. The irrigation interval for a field is directly affected by the capacity (water volume per land area per unit time) of the irrigation system.

The amount of water depletion at any specific time is the amount of water required to refill the current crop root zone to field capacity (upper limit of soil water storage). However, computation of the water depleted in a soil profile is more convenient than determining the water remaining for many practical applications. From the perspective of practical irrigation management, using FC_{obs} and managing for depletion instead of actual soil water content resulted in a considerable reduction in uncertainty (figs. 5 and 6). This method removes most of the uncertainty from sensor-to-sensor variability and removes much of the uncertainty from spatial variability of soil properties.

Implications for Global Water Security

Water security should be understood as the tolerable water-related risk to society (Grey et al., 2013). The challenge of optimum allocation of water resources, if left unaddressed, will hinder the ability to produce food and generate energy, which would further pose a risk to global food markets and hobble economic growth. One way to improve water security on a large scale is to improve irrigation management on a field scale. In general, while it is desirable to make irrigation prescriptions with high accuracy, it is difficult to ascertain soil moisture, rainfall, irrigation depth, evapotranspiration, and other components of the soil water balance. For example, in surface irrigation systems, the net depth of water applied is the largest source of uncertainty in

the soil water balance, based on the results of a study by Jensen and Wright (1978). While soil water content can be measured directly, there are also significant sources of uncertainty when using soil water sensors. In this study, this uncertainty was reduced to a greater extent when the depth of water depletion was evaluated. It was found that managing for depletion based on FC_{obs} had much less uncertainty. This would give producers much more confidence in their irrigation decision-making and could potentially reduce water use by reducing over-irrigation. It also reduces the need for producers to determine a precise calibration for their particular soil types. To further reduce the uncertainty, it would be useful to select representative sites and perform periodic monitoring of the same site.

In the next decade, many countries will experience water problems, such as shortages, poor water quality, and floods. If water resources are not more efficiently managed, freshwater availability will not keep up with demand (ICA, 2012). Technological advances, such as optimum allocation of water resources in agriculture, will have an important impact on water supply and demand in the coming years. The results of this study have further implications when considering the opportunity for variable-rate irrigation. As technology costs continue to decrease, the ability to manage sub-field areas based on varying available water capacities may become more attractive. The Yutan soil type dominated this study field (>20 ha), and the Fillmore soil type comprised the least amount of the total field area (<2 ha). Had properly calibrated sensors been installed in a zone containing the Yutan soil, little error would likely have been introduced to zones containing the Fillmore soil. However, improperly calibrated sensors in the Fillmore zone could adversely affect the majority of the field in terms of irrigation management for better allocation of water based on required depth and timing.

CONCLUSIONS

The performance of a recently developed capacitance and frequency domain technology based EM sensor (GS-1) was analyzed in a laboratory experiment conducted on soils taken from a center-pivot field in Mead, Nebraska. For both disturbed and undisturbed soil structures, a linear calibration equation was statistically significant ($p < 0.05$), with a slope close to unity for the undisturbed soil structure and $RMSD_L$ of 0.053 and 0.023 $m^3 m^{-3}$ for the disturbed and undisturbed soil structures, respectively. This implies that it would be appropriate for producers to test the applicability of a soil moisture sensor in the field rather than bringing soil into the laboratory and calibrating the sensor. The response of Yutan and Fillmore soil texture classes had better correlation (slope closer to 1) in the undisturbed soil structure. The reported $RMSD_L$ values for Yutan and Fillmore were 0.046 and 0.035 $m^3 m^{-3}$, respectively, for the disturbed soil structure and 0.028 and 0.023 $m^3 m^{-3}$, respectively, for the undisturbed soil structure. In addition, the response of the GS-1 sensor was significantly different ($p = 0.0398$) in the disturbed soil structure, but it was not significantly different ($p = 0.10$) in the undisturbed soil structure. Finally, the sensor response for the different soil types varied across the different soil structures.

For irrigation management, the results of this study should not be generalized or extrapolated beyond the range of the sensor responses in this experiment. In general, the uncertainty in the estimation of soil water depth was higher than the uncertainty in soil water depletion. This would lead to the determination of water demand at a specific site with better precision and could potentially avoid over-watering of the crop. Technological advances that could reduce the amount of water needed for agriculture would offer the greatest relief from water shortages (ICA, 2012). The uncertainty in both root zone water depth and depletion was lower using the undisturbed soil structure calibration for both Yutan and Fillmore soil types. In the future, universal calibrations could be developed to enhance the applicability of soil moisture sensors for efficient irrigation management and optimum utilization of water resources.

ACKNOWLEDGEMENTS

The funding for this research was provided by a grant from the USDA-NIFA Agricultural and Food Research Initiative (Award No. 2017-67021-26249) and Graduate Student Support from the Robert B. Daugherty Water for Food Global Institute at the University of Nebraska. Additional support was received from the USDA-NIFA Hatch Act (Accession No. 1009760) and the Department of Biological Systems Engineering at the University of Nebraska-Lincoln. The authors thank Dr. Burdette Barker for input in the experimental design, Alan L. Boldt and Jingjing Li for assistance with the data collection, and Dr. Tsz Him Lo and Dr. George Meyer for reviewing an earlier version of the manuscript.

REFERENCES

Adeyemi, O., Norton, T., Grove, I., & Peets, S. (2016). Performance evaluation of three newly developed soil moisture sensors. *Proc. CIGR-AgEng Conf.* (pp. 26-29). Retrieved from https://www.cabdirect.org/cabdirect/abstract/20183376956

Andrade-Sánchez, P., Upadhyaya, S. K., Aguera-Vega, J., & Jenkins, B. M. (2004). Evaluation of a capacitance-based soil moisture sensor for real-time applications. *Trans. ASAE, 47*(4), 1281-1287. https://doi.org/10.13031/2013.16562

Barker, J. B., Franz, T. E., Heeren, D. M., Neale, C. M., & Luck, J. D. (2017). Soil water content monitoring for irrigation management: A geostatistical analysis. *Agric. Water Mgmt., 188*, 36-49. https://doi.org/10.1016/j.agwat.2017.03.024

Baumhardt, R. L., Lascano, R. J., & Evett, S. R. (2000). Soil material, temperature, and salinity effects on calibration of multisensor capacitance probes. *SSSA J., 64*(6), 1940-1946. https://doi.org/10.2136/sssaj2000.6461940x

Cobos, D. (2016). Measurement volume of Decagon volumetric water content sensors. Pullman, WA: Decagon Devices, Inc. Retrieved from http://manuals.decagon.com/Application Notes/14955_VWC Sensor Measurement Volumes_Web.pdf

Datta, S., Taghvaeian, S., Ochsner, T. E., Moriasi, D., Gowda, P., & Steiner, J. L. (2018). Performance assessment of five different soil moisture sensors under irrigated field conditions in Oklahoma. *Sensors, 18*(11), 3786. https://doi.org/10.3390/s18113786

Dobriyal, P., Qureshi, A., Badola, R., & Hussain, S. A. (2012). A

review of the methods available for estimating soil moisture and its implications for water resource management. *J. Hydrol., 458-459*, 110-117. https://doi.org/10.1016/j.jhydrol.2012.06.021

Evett, S. R. (2007). Soil water and monitoring technology. In *Irrigation of agricultural crops* (2nd Ed.). Agronomy Monograph No. 30. Madison, WI: ASA-CSSA-SSSA. https://doi.org/10.2134/agronmonogr30.2ed.c2

Francesca, V., Osvaldo, F., Stefano, P., & Paola, R. P. (2010). Soil moisture measurements: Comparison of instrumentation performances. *J. Irrig. Drain. Eng., 136*(2), 81-89. https://doi.org/10.1061/(ASCE)IR.1943-4774.0000130

Gabriel, J. L., Lizaso, J. I., & Quemada, M. (2010). Laboratory versus field calibration of capacitance probes. *SSSA J., 74*(2), 593-601. https://doi.org/10.2136/sssaj2009.0157

Geerts, S., & Raes, D. (2009). Deficit irrigation as an on-farm strategy to maximize crop water productivity in dry areas. *Agric. Water Mgmt., 96*(9), 1275-1284. https://doi.org/10.1016/j.agwat.2009.04.009

Geesing, D., Bachmaier, M., & Schmidhalter, U. (2004). Field calibration of a capacitance soil water probe in heterogeneous fields. *Soil Res., 42*(3), 289-299. https://doi.org/10.1071/SR03051

Goswami, M. P., Montazer, B., & Sarma, U. (2019). Design and characterization of a fringing field capacitive soil moisture sensor. *IEEE Trans. Instrum. Meas., 68*(3), 913-922. https://doi.org/10.1109/TIM.2018.2855538

Grey, D., Garrick, D., Blackmore, D., Kelman, J., Muller, & Sadoff, C. (2013). Water security in one blue planet: Twenty-first century policy challenges for science. *Phil. Trans. Royal Soc. A, 371*(2002), 20120406. https://doi.org/10.1098/rsta.2012.0406

Groves, S. J., & Rose, S. C. (2004). Calibration equations for Diviner 2000 capacitance measurements of volumetric soil water content of six soils. *Soil Use Mgmt., 20*(1), 96-97. https://doi.org/10.1111/j.1475-2743.2004.tb00343.x

Haberland, J., Galvez, R., Kremer, C., & Carter, C. (2014). Laboratory and field calibration of the Diviner 2000 probe in two types of soil. *J. Irrig. Drain. Eng., 140*(4), 2-7. https://doi.org/10.1061/(ASCE)IR.1943-4774.0000687

Hignett, C., & Evett, S. R. (2008). Chapter 1: Direct and surrogate measures of soil water content. In *Field estimation of soil water content: A practical guide to methods, instrumentation, and sensor technology* (pp. 1-21). Vienna, Austria: International Atomic Energy Agency.

Huang, J., McBratney, A. B., Minasny, B., & Triantafilis, J. (2017). Monitoring and modeling soil water dynamics using electromagnetic conductivity imaging and the ensemble Kalman filter. *Geoderma, 285*, 76-93. https://doi.org/10.1016/j.geoderma.2016.09.027

ICA. (2012). Global water security. Intelligence Community Assessment ICA-2012-08. Washington, DC: Office of the Director of National Intelligence. Retrieved from https://www.dni.gov/files/documents/Special Report_ICA Global Water Security.pdf

Jensen, M. E., & Wright, J. L. (1978). The role of evapotranspiration models in irrigation scheduling. *Trans. ASAE, 21*(1), 82-87. https://doi.org/10.13031/2013.35254

Kelleners, T. J., Soppe, R. W., Ayars, J. E., & Skaggs, T. H. (2004). Calibration of capacitance probe sensors in a saline silty clay soil. *SSSA J., 68*(3), 770-778. https://doi.org/10.2136/sssaj2004.7700

King, B. A., Stark, J. C., & Wall, R. W. (2006). Comparison of site-specific and conventional uniform irrigation management for potatoes. *Appl. Eng. Agric., 22*(5), 677-688. https://doi.org/10.13031/2013.22000

Kizito, F., Campbell, C. S., Campbell, G. S., Cobos, D. R., Teare, B. L., Carter, B., & Hopmans, J. W. (2008). Frequency, electrical conductivity, and temperature analysis of a low-cost capacitance soil moisture sensor. *J. Hydrol., 352*(3), 367-378. https://doi.org/10.1016/j.jhydrol.2008.01.021

Lea-Cox, J. D., Williams, J., & Mellano, M. A. (2018). Optimising a sensor-based irrigation protocol for a large-scale cut-flower operation in southern California. *Acta Hort., 1197*( ), 219-225. https://doi.org/10.17660/ActaHortic.2018.1197.29

Lo, T. H., Heeren, D. M., Mateos, L., Luck, J. D., Martin, D. L., Miller, K. A., ... Shaver, T. M. (2017). Field characterization of field capacity and root zone available water capacity for variable-rate irrigation. *Appl. Eng. Agric., 33*(4), 559-572. https://doi.org/10.13031/aea.11963

Logsdon, S. D. (2009). CS616 calibration: Field versus laboratory. *SSSA J., 73*(1), 1-6. https://doi.org/10.2136/sssaj2008.0146

Majone, B., Viani, F., Filippi, E., Bellin, A., Massa, A., Toller, G., ... Salucci, M. (2013). Wireless sensor network deployment for monitoring soil moisture dynamics at the field scale. *Procedia Environ. Sci., 19*, 426-435. https://doi.org/10.1016/j.proenv.2013.06.049

Martin, D. L., Stegman, E. C., & Fereres, E. (1990). Irrigation scheduling principles. In *Management of farm irrigation systems* (pp. 155-177). St. Joseph, MI: ASAE.

Mittelbach, H., Lehner, I., & Seneviratne, S. I. (2012). Comparison of four soil moisture sensor types under field conditions in Switzerland. *J. Hydrol., 430-431*, 39-49. https://doi.org/10.1016/j.jhydrol.2012.01.041

Namdar-Khojasteh, D., Shorafa, M., & Heidari, A. (2012). Estimating soil water content from permittivity for different mineralogies and bulk densities. *SSSA J., 76*(4), 1149-1158. https://doi.org/10.2136/sssaj2011.0144

Ojo, E. R., Bullock, P. R., & Fitzmaurice, J. (2014). Field performance of five soil moisture instruments in heavy clay soils. *SSSA J., 79*(1), 20-29. https://doi.org/10.2136/sssaj2014.06.0250

Ojo, E. R., Bullock, P. R., L'Heureux, J., Powers, J., McNairn, H., & Pacheco, A. (2015). Calibration and evaluation of a frequency domain reflectometry sensor for real-time soil moisture monitoring. *Vadose Zone J., 14*(3). https://doi.org/10.2136/vzj2014.08.0114

Paige, G. B., & Keefer, T. O. (2008). Comparison of field performance of multiple soil moisture sensors in a semi-arid rangeland. *JAWRA, 44*(1), 121-135. https://doi.org/10.1111/j.1752-1688.2007.00142.x

Provenzano, G., Rallo, G., & Ghazouani, H. (2016). Assessing field and laboratory calibration protocols for the Diviner 2000 probe in a range of soils with different textures. *J. Irrig. Drain. Eng., 142*(2), 1-12. https://doi.org/10.1061/(ASCE)IR.1943-4774.0000950

Romano, N., & Santini, A. (2002). The soil solution phase. In *Methods of soil analysis: Part 4 physical methods* (Vol. 5, pp. 721-738). Madison, WI: SSSA.

Rudnick, D. R., Djaman, K., & Irmak, S. (2015). Performance analysis of capacitance and electrical resistance-type soil moisture sensors in a silt loam soil. *Trans. ASABE, 58*(3), 649-665. https://doi.org/10.13031/trans.58.10761

Santhosh, L. G., Lakshmikanthan, P., & Babu, G. L. (2017). Laboratory investigation of large-scale MSW reactor under anaerobic conditions. *Indian Geotech. J., 47*(4), 395-409. https://doi.org/10.1007/s40098-017-0263-5

Saxton, K. E., & Rawls, W. J. (2006). Soil water characteristic estimates by texture and organic matter for hydrologic solutions. *SSSA J., 70*(5), 1569-1578. https://doi.org/10.2136/sssaj2005.0117

Singh, J., Lo, T., Rudnick, D. R., Dorr, T. J., Burr, C. A., Werle, R., ... Muñoz-Arriola, F. (2018). Performance assessment of factory and field calibrations for electromagnetic sensors in a loam soil.

Agric. Water Mgmt., 196, 87-98. https://doi.org/10.1016/j.agwat.2017.10.020
Singh, J., Lo, T., Rudnick, D. R., Irmak, S., & Blanco-Canqui, H. (2019). Quantifying and correcting for clay content effects on soil water measurement by reflectometers. *Agric. Water Mgmt., 216*, 390-399. https://doi.org/10.1016/j.agwat.2019.02.024
Sui, R. (2017). Irrigation scheduling using soil moisture sensors. *J. Agric. Sci., 10*(1). https://doi.org/10.5539/jas.v10n1p1
Varble, J. L., & Chávez, J. L. (2011). Performance evaluation and calibration of soil water content and potential sensors for agricultural soils in eastern Colorado. *Agric. Water Mgmt., 101*(1), 93-106. https://doi.org/10.1016/j.agwat.2011.09.007
Vaz, C. M., Jones, S., Meding, M., & Tuller, M. (2013). Evaluation of standard calibration functions for eight electromagnetic soil moisture sensors. *Vadose Zone J., 12*(2). https://doi.org/10.2136/vzj2012.0160